

THREE-DIMENSIONAL RECONSTRUCTED POROUS MEDIA.  
APPLICATION TO THE STUDY OF TRANSPORT MECHANISMS  
IN SANDSTONES

Adler P.M.\*, Jacquin C.G.\*\* ,Rahon D.\*\*\*

\* Laboratoire d'Aérothermique du C.N.R.S., Meudon, France

\*\* Institut Français du Pétrole, Rueil Malmaison, France

\*\*\*B.E.I.C.I.P., Rueil Malmaison, France

Abstract 3-dimensional random porous structures are generated, which share the same statistical properties as the pore space of real materials observed on thin sections. It is then possible to simulate transport phenomena in these reconstructed media, and to calculate the permeability and the formation factor. The methodology is illustrated on an example: the Fontainebleau sandstone.

INTRODUCTION

Petrophysical measurements, on samples of porous rocks, are classically performed in the context of Core Analysis (porosity, permeability, formation factor).

On the other hand, qualitative and quantitative informations are obtained from the study of thin sections of the same materials.

The purpose of this paper is to present an attempt to establish a link between these two aspects, and to try to solve a long standing problem: to deduce the transport properties of a 3-dimensional sample (plug) from the corresponding geometrical structures of the pore space, which can be observed and characterised in 2 dimensions (thin sections).

This problem is difficult for two main reasons:

- it is hard to describe quantitatively the 3-D geometry of the medium in a realistic manner, without introduction of artificial models and parameters (see Adler (1989)).
- the partial differential equations corresponding to these transport phenomena are not easy to solve, except numerically.

This paper is organized as follows:

- presentation of the material and of the experimental data, obtained on the plugs,
- analysis of the images of thin sections,
- simulation of the porous media,
- simulation of the transport phenomena in the reconstructed samples,
- results and comments.

A general conclusion ends up the paper.



*Figure 1.* Thin section. Fontainebleau sandstone

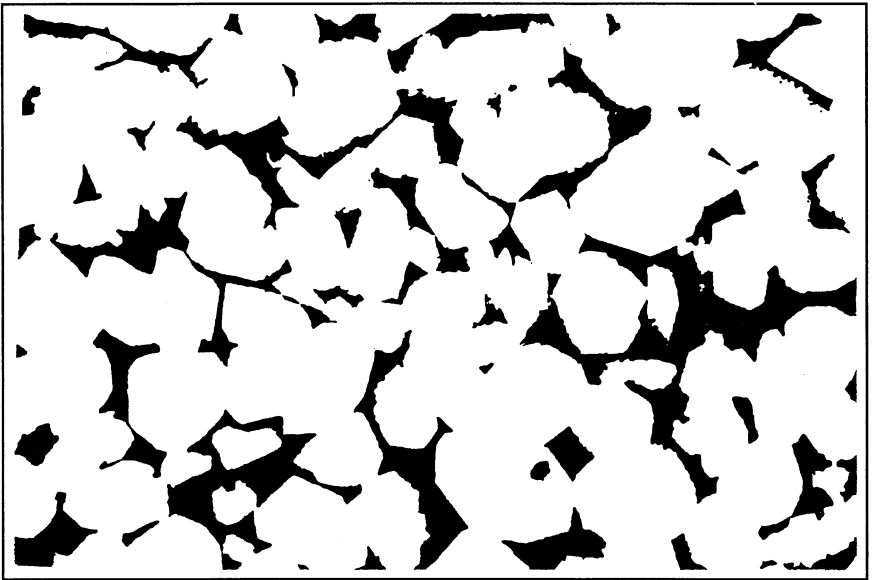


*Figure 2.* Black-and-white transformed image  
pore space : black    solid phase : white

## MATERIAL AND PETROPHYSICAL DATA

The geological material selected for this study is the Fontainebleau sandstone, which is a rather simple natural porous rock (see Jacquin (1964), Jacquin and Adler (1987)):

- it is made of quartz grains, without any clay mineral;
- the grain size distribution is very well sorted (grain size about 250 microns);
- the originally deposited material (sand) has been consolidated by a quartz diagenetic cement;
- the resulting sandstone displays a rather simple geometry, with only intergranular connected porosity;
- depending on the amount of cement, the porosity varies in a large range (3 to 35%), while the same structure is globally conserved.

Classical laboratory techniques were used to obtain the petrophysical characteristics of a large number of plugs of this sandstone:

- porosity  $\emptyset$ ,
- permeability  $K$ ,
- formation factor  $F$ .

The results were presented in Jacquin (1964). A rather good porosity-permeability correlation was observed; nevertheless large fluctuations exist, and the permeability may vary by a factor of 10 for plugs presenting the same porosity. A good correlation was also obtained between porosity and formation factor. In both cases, the correlations can be approximated by power laws:

$$K = \beta \cdot \emptyset^n \quad \text{with } n \sim 4.15 \quad (1)$$

$$F = \gamma \cdot \emptyset^m \quad \text{with } m \sim 1.5 \quad (2)$$

## THIN SECTIONS ANALYSIS

The pore space has been injected with a red epoxy resin, and it can be observed without difficulty through a microscope. Nevertheless, the pictures obtained from thin sections cannot be quantitatively analysed directly due to the hardware, which is sensitive only to grey levels and is unable to make the selection between real informations, (pore space or solid phase), and local artefacts (Figure 1).

These artefacts are manually eliminated directly on the picture, in order to obtain black-and-white images (Figure 2).

The automatic image analyser operates a "discretization" of these black-and-white pictures (Figure 3), and registers the corresponding 2-D phase function, defined as follows:

$$Z(x) = \begin{cases} 1 & \text{if } x \text{ belongs to the pores} \\ 0 & \text{if } x \text{ belongs to the solid} \end{cases} \quad (3)$$

where  $x$  denotes the position with respect to an arbitrary origin.

It is then possible to obtain two statistical averages

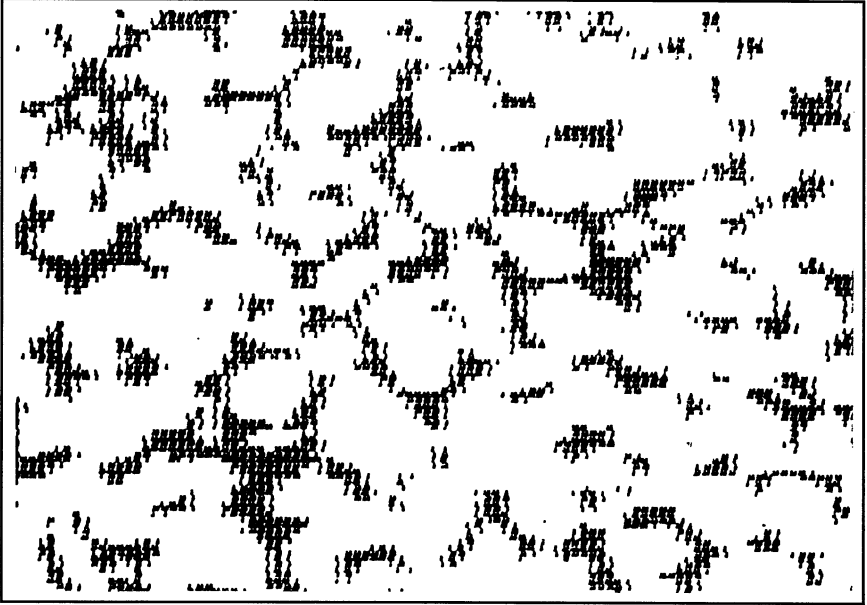


Figure 3. Discretized image. Fontainebleau sandstone

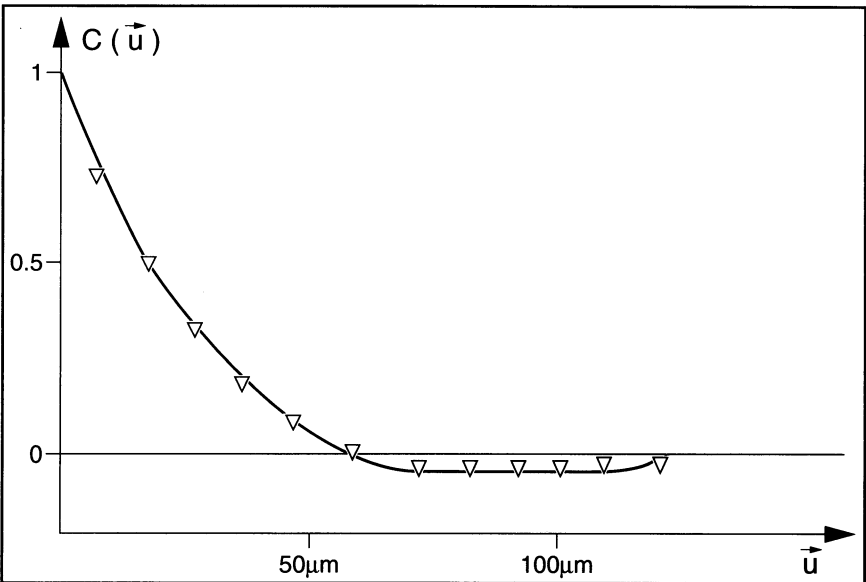


Figure 4. Experimental correlation function obtained on a thin section. Fontainebleau sandstone

which characterize the pore space observed on the section:

-the porosity:

$$\emptyset = \overline{Z(x)} \quad (4)$$

-the correlation function:

$$C(u) = \frac{\overline{(Z(x) - \emptyset)(Z(x+u) - \emptyset)}}{\emptyset(1 - \emptyset)} \quad (5)$$

where u indicates a translation.

The surface integrations corresponding to the equations (4) and (5) are done by the software, which performs algebraic operations and intersections of images.

It should be noticed that this corresponds to the replacement of statistical averages by surface averages; this is justified for this Fontainebleau sandstone, which is considered as homogeneous and isotropic at the scale of a thin section (see Jacquin and Adler(1987)).

Figure 4 presents an example of a correlation function obtained by this procedure. The shape of these experimental correlation functions indicate that a "correlation length" L could be introduced.

#### RECONSTRUCTION OF THE 3-D POROUS STRUCTURES

Let us first indicate the purpose of this section: we want to generate a 3-D porous medium with a given porosity and with a given correlation function.

This medium is constructed in a discrete manner, being composed of N.N.N elementary cubic cells of size a; these cells correspond either to solid or to fluid. A schematic illustration is given in Figure 5. The size of the generated sample is N.a and, as it is standard, we will consider periodic boundary conditions.

In order to obtain a reconstructed 3-D geometry, representative of the real one, certain conditions should be satisfied:

-the size of the generated sample has to be large enough, compared to the correlation length of the medium:

$$N.a \gg L \quad (6)$$

-the size of the elementary cells has to be small enough, such that two adjacent cells are well-connected:

$$a \ll L \quad (7)$$

The stronger these inequalities are verified, the better is the result; but other considerations (essentially limitations of computing time) have to be taken in account. An acceptable compromise could be empirically obtained.

The method we use to generate the reconstructed media corresponds to the specialisation to isotropic geometries of an algorithm due to Quiblier(1984). This algorithm is an extension to 3-D of a 2-D scheme (Joshi(1974)).

The details of the reconstruction process will not be presented here (see Adler et al.(1990)). It can be summarized as follows:

1-generate a gaussian random field  $X(x)$ ; the random variables  $X(x)$  are independent and normally distributed, with a mean value equal to zero and a variance equal to unity;  
 2-calculate a new gaussian random field  $Y(x)$ , by a linear combination of the variables  $X(x)$ :

$$Y(x) = \sum \alpha(u) \cdot X(x) \quad (8)$$

where  $u$  indicates a translation and  $\alpha$  are coefficients. These random variables  $Y(x)$  have a standard, normal, distribution, with a distribution function  $P(y)$ , but they are spatially correlated. With an appropriate choice of the coefficients, their correlation function  $Cy(u)$  can be fitted to a chosen correlation function.

3-apply to  $Y(x)$  a transformation  $G$ , in order to obtain a discrete-valued field  $Z(x)$ :

$$Z = G(Y) \quad (9)$$

$G$  being defined by:

$$Z = \begin{cases} 1 & \text{if } P(y) < \emptyset \\ 0 & \text{otherwise} \end{cases} \quad (10)$$

With this condition, the average value of  $Z(x)$  is equal to the porosity  $\emptyset$ , and its variance is equal to  $\emptyset(1-\emptyset)$ . The corresponding correlation function is related to  $Cy(u)$ .

Practically, when one wants to simulate a given porous structure, with a given porosity, and a given correlation function, a preliminary step is to solve the "inverse problem": to determine the coefficients  $\alpha(u)$  of equation (8).

#### TRANSPORT PHENOMENA IN THE RECONSTRUCTED POROUS MEDIA

Once a sample is generated, transport phenomena in the pore space are simulated numerically.

Incompressible fluid flow-Permeability:

The flow of an incompressible newtonian fluid at low  $Re$  (Reynolds number), is governed by the Stokes equations:

$$\nabla p = \mu \cdot \nabla^2 v \quad (11a)$$

$$\nabla \cdot v = 0 \quad (11b)$$

where  $p, v$  and  $\mu$  are, respectively, the pressure, the velocity and the viscosity.

The boundary conditions are:

$$v \text{ spatially periodic} \quad (12a)$$

$$v = 0 \text{ on the wetted solid} \quad (12b)$$

$$\text{average pressure gradient} = \text{a prescribed value} \quad (12c)$$

The numerical 3-D scheme used is described in Lemaitre and Adler (1990). In essence, the problem is replaced by a compressible unsteady-state flow problem which converges towards the incompressible steady one.

The equations are solved by an alternating-direction-implicit method.

From the calculated velocity field it is easy to deduce the global flow rate corresponding to the prescribed macroscopic pressure gradient and, applying the Darcy law, to obtain the permeability.

Electrical conductivity-Formation factor:

The electrical conductivity of the reconstructed samples is calculated by a numerical scheme, similar to the one we used for the evaluation of permeability. The system of equations is rather simple here; there is no boundary condition to impose on the solid phase (no condition similar to equation 12b) and the local phenomena are governed by a Laplace equation, in place of Stokes equation. The problem is solved by a conjugate gradient method.

Unsteady state fluid flow-Dynamic permeability:

When small amplitude oscillations (pulsation =  $\omega$ ) are imposed to the macroscopic pressure gradient, a generalized Darcy law is introduced (see Auriault et al. (1985)), of the form:

$$V(\omega) = - \frac{K(\omega)}{\mu} P(\omega) \quad (13)$$

with:

$$\begin{aligned} V(\omega) & \text{ average flow velocity} \\ P(\omega) & \text{ macroscopic pressure gradient} \\ \text{and a generalized (or dynamic) permeability:} \\ K(\omega) & = K_r(\omega) + i.K_i(\omega) \end{aligned} \quad (14)$$

This corresponds to the fact that:

- at low frequencies, the viscous forces govern the pressure drop ( $K_r$ , real part of  $K$ ),
- at high frequencies, the inertial forces dominate ( $K_i$ , imaginary part of  $K$ ).

This phenomenon has been observed experimentally in very specific situations (see Auriault et al. (1985), Ping and Min-Yau Zhou (1988), Charlaix et al. (1988)), but does not correspond to classical measurements of conventional core analysis.

It could be instructive to observe these effects in complicated natural porous structures, and we developed a model to simulate the phenomena in a reconstructed geometry (Rahon (1990)). The numerical method used is the conjugate gradient, and the validity of the model was tested on simple geometries (analytical solutions exist for cylindrical ducts and slots).

## RESULTS AND DISCUSSION

The results are presented on figures 6 to 10, and general comments are given hereafter.

Geometry of the reconstructed samples:

A specific software was adapted to obtain good representations of the simulated geometries, with the possibility to rotate the object. Figure 6 shows an example of a re-

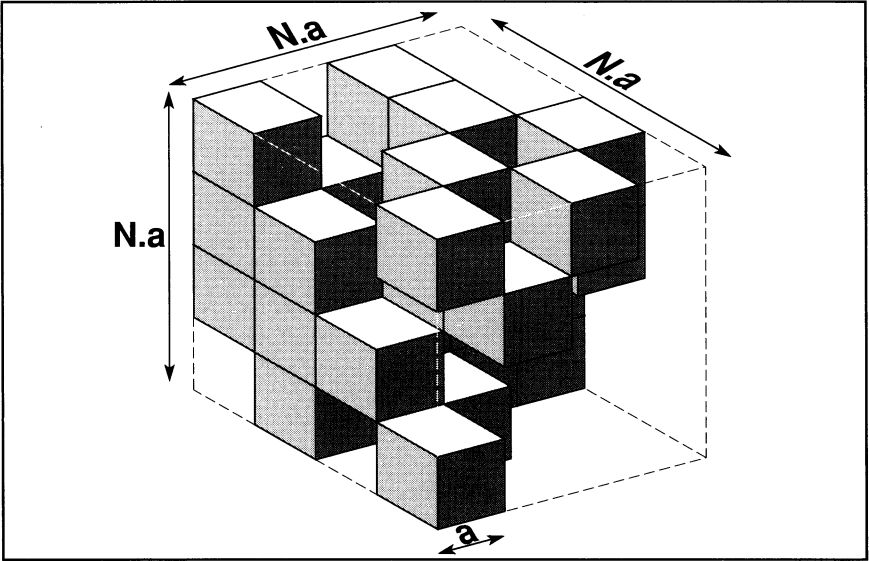


Figure 5. Schematic illustration of the reconstructed geometry

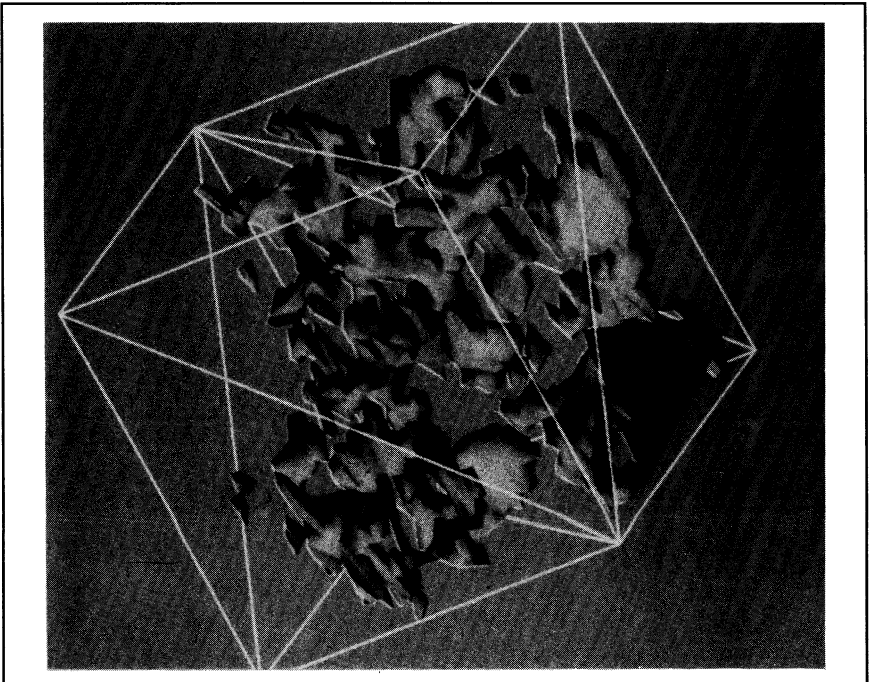


Figure 6. Example of a reconstructed sample



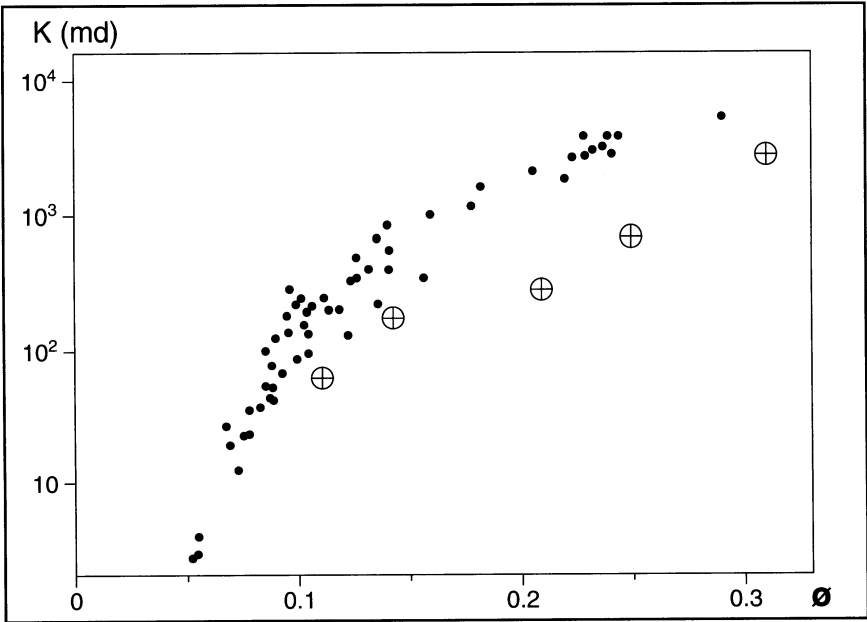


Figure 7. Permeability as a function of porosity. Fontainebleau sandstone  
 • experimental data (Jacquin - 1964)    ⊕ calculated on reconstructed samples

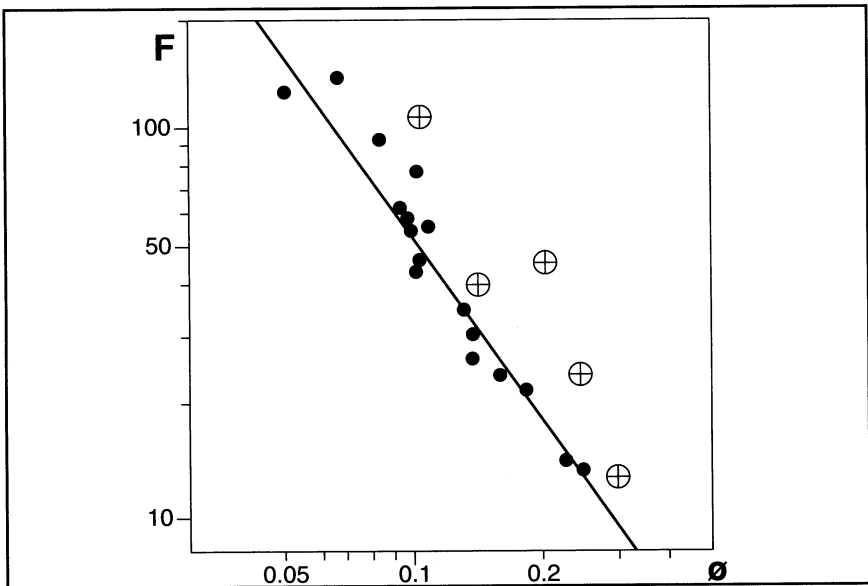


Figure 8. Formation factor as a function of porosity. Fontainebleau sandstone  
 • experimental data (Jacquin - 1964)    ⊕ calculated on reconstructed samples

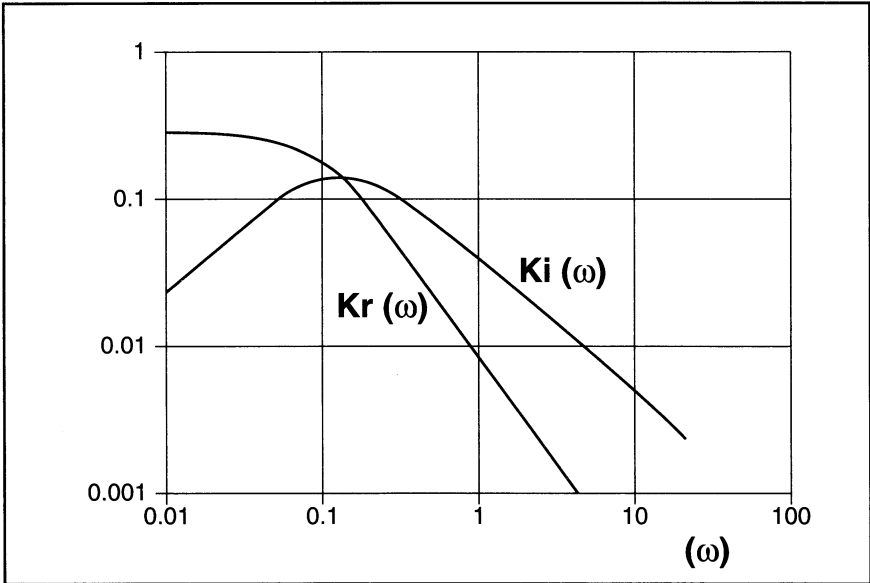


Figure 9. Complex dynamic permeability  
Sample with one fracture

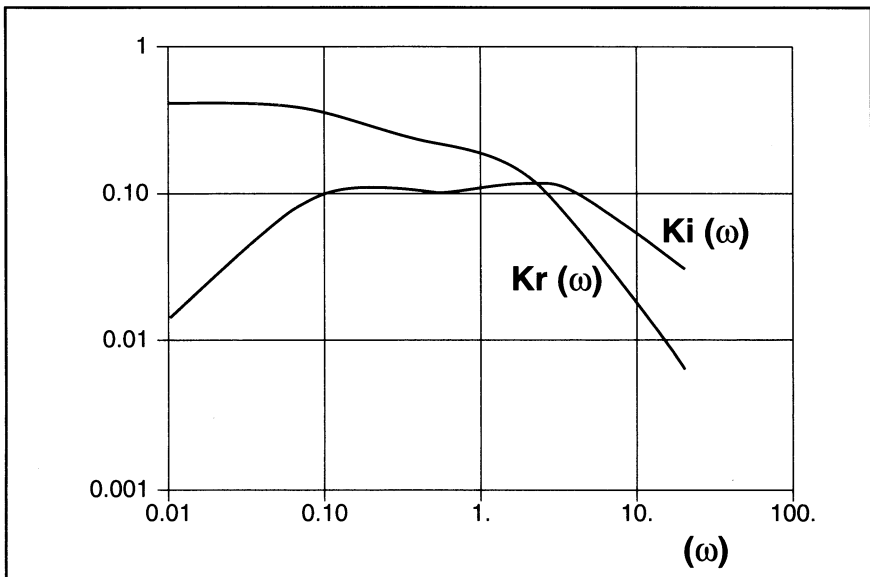


Figure 10. Complex dynamic permeability  
Reconstructed sample with two different characteristic length scales

constructed sample. It is composed of about 500,000 elementary cubic cells.

Looking at the statistical properties of simulated structures (porosity and correlation function), it was verified that the agreement with the experimental data obtained on the thin sections is good. Nevertheless, the influence of the number of simulations is evident, and one needs to generate at least 5 configurations for one set of data.

#### Permeability:

For a given set of data obtained on a thin section (porosities: 11%, 14%, 21% and 31%), a certain number of configurations are simulated (minimum: 7; maximum: 28).

It is observed that a certain number of configurations do not percolate, i.e. have a zero permeability. This is not surprising, and corresponds to statistical fluctuations of the geometry. The smaller the porosity, the larger these fluctuations are, due to computing time limitations, we did not study situations corresponding to porosities lower than 10%.

65 reconstructed samples were generated, and their permeabilities were calculated. For a given porosity, the average permeability is calculated and compared to the experimental data. The results are shown in figure 7.

#### Formation factor:

The methodology is similar to the one applied for permeability; the results are presented and compared to the laboratory data in figure 8.

#### Dynamic permeability:

The phenomena leading to the introduction of a "dynamic permeability" were not systematically investigated.

Specific situations were examined; examples of results obtained are presented in figures 9 and 10; they correspond, respectively:

- to a simple case, where an analytical solution exists: one slot, which could more or less represent a fracture.
- to a more complex geometry, with different characteristic length scales.

#### CONCLUSIONS

It may be the right place here to make some comments on the methodology used and on the quality of the results.

First, it is essential to remind that the simulation of the geometries and of the transport processes do not involve any hidden adjusted parameter; every quantity introduced in the models is measured on a natural rock.

Concerning the results obtained, we observe that the shapes of the experimental porosity-permeability and

porosity-formation factor correlations are predicted in a rather good way by the simulations. The calculated values of permeabilities differ by about a factor 5 from the measured values, indicating something like a systematic "error". The same observations can be made for the formation factor.

These observed discrepancies between the calculated and the experimental values result from three facts:  
 -the two statistical characteristics which are taken in account (porosity and correlation function) may not be sufficient to describe with a good precision the geometry of real media;  
 -the discretization of the pore space introduces an artificial "roughness" of the solid-fluid interface, which results in an underestimation of the permeabilities, and in an overestimation of the formation factors.  
 -finite-size effects may be important, and the statistical fluctuations could be minimized on larger samples.

These two last points result only from technological limitations (computer power).

More generally, this work leads to outline the importance of the geometry, which is very complex in natural porous rocks.

#### REFERENCES

- ADLER, P.M. (1989) Flow in Porous Media-In: The "Fractal Approach to Heterogeneous Chemistry", edited by D. Avnir, Wiley, New York.
- ADLER, P.M., JACQUIN, C.G. and QUIBLIER, J.A. (1990) Flow in Simulated Porous Media. *International Journal of Multiphase Flow* Vol. 16, pp. 691-712.
- AURIAULT, J.L., BORNE, L. and CHAMBON, R. (1985) Dynamics of porous saturated media, checking of the generalized Darcy law. *Journal of the Acoustical Society of America* Vol. 77, pp. 1641-1650.
- CHARLAIX, E., KUSCHNICK, A.P. and STOKES, J.P. (1988) Experimental Study of Dynamic Permeability, in Porous Media *Physical Review Letters* Vol. 61, pp. 1595-1598.
- JACQUIN, C.G. (1964) Corrélations entre la perméabilité et les caractéristiques géométriques du grès de Fontainebleau. *Revue de l'Institut Français du Pétrole* Vol. 19, pp. 921-937.
- JACQUIN, C.G. and ADLER, P.M. (1987) Fractal porous media-II Geometry of porous geological structures. *Transport in Porous Media* Vol. 2, pp. 571-596.
- JOSHI, M. (1974) Thesis - University of Kansas, Lawrence, Kansas.
- LEMAITRE, R. and ADLER, P.M. (1990) Fractal porous media. IV Three dimensional Stokes flow through random media and regular fractals. (accepted for publication).

- PING SHENG and MIN-YAU ZHOU (1988) Dynamic Permeability  
in Porous Media.  
*Physical Review Letters*  
Vol.61,pp.1591-1594.
- QUIBLIER, J.A. (1984) A new three-dimensional modeling technique for studying porous media .  
*Journal of Colloid and Interface Science*  
Vol.98,pp.84-102.
- RAHON, D. (1990) Conception et mise au point d'un programme de calcul de la perméabilité de milieux poreux simulés, en régime dynamique-Institut Français du Pétrole, internal report 38448.

